

Supporting Information

Solid-State Self Carbo-Passivation for Refurbishing Colloidal Dispersivity of Catalytic Silica Nanoreactors

*Jeong Hun Choi,^{‡ab} Nitee Kumari,^{‡ab} Anubhab Acharya,^{ab} Amit Kumar,^{ab} Sanghwang Park,^b Dongyeon Ro,^b Jongcheol Seo,^b Eunhye Lee,^{cd} Jee Hwan Bae,^e Dong Won Chun,^f Kyungtaek Oh,^b Sunmin Ryu,^b In Su Lee^{*abg}*

^aCreative Research Initiative Center for Nanospace-confined Chemical Reactions (NCCR), Pohang University of Science and Technology (POSTECH), Pohang 37673, Korea

^bDepartment of Chemistry, Pohang University of Science and Technology (POSTECH), Pohang 37673, Korea

^cEnergy Materials Research Center, Korea Institute of Science and Technology (KIST), Seoul 02792 (Korea)

^dDepartment of Materials Science and Engineering, Yonsei University

^eAdvanced Analysis and Data Center, Korea Institute of Science and Technology

^fDepartment of Materials Science and Engineering, Pohang University of Science and Technology (POSTECH), Pohang, 37673 Republic of Korea

^gInstitute for Convergence Research and Education in Advanced Technology (I-CREATE), Yonsei University, Seoul 03722 (Korea)

[‡]These authors contributed equally to this work.

*Correspondence: insulee97@postech.ac.kr (I. S. L.)

Movie S1: Liquid-Cell TEM movie (150 nm-low magnification) showing well-dispersed Pd₂Si@SiO₂ NPs

Movie S2: NTA video of colloidal solution of **Pd₂Si@SiO₂** in water after 24 h. Videos were taken at 24 fps.

S1. Material and Methods

Materials: IGEPAL CO-520 [polyoxyethylene (5) nonylphenylether, Aldrich], IGEPAL CO-720 [polyoxyethylene (12) nonylphenylether, Aldrich], tetraethyl orthosilicate (TEOS, 98%, Acros), N-[3-(trimethoxysilyl)propyl]ethylenediamine (TMSD, Aldrich, 97%), aqueous ammonia (NH₃, 28~30%, Samchun Chem.), sodium tetrachloropalladate trihydrate (Na₂PdCl₄·3H₂O, 99%, Strem chem.), iron chloride (Fe(Cl)₃, ACROS), isobutyl(trimethoxy)silane (97%, Aldrich) and dopamine hydrochloride (Aldrich) were purchased and used without further purification.

S2. Instruments and Characterization.

Transmission electron microscopy (TEM) was conducted with a JEM-2100 (JEOL) instrument at acceleration voltage of 200 kV for imaging and a JEM-2100F (JEOL) instrument at an acceleration voltage of 200 kV for STEM-EDS elemental mapping, line profiling module. 10 µl of sample dispersed in 1mL of ethanol was dropped on a TEM grid and dried in air for 30 min before TEM characterizations. Copper mesh TEM grids with carbon film and silicon nitride TEM grids were used for TEM characterizations. Zeta potentials were measured using Malvern Zetasizer (Malvern Panalytical) 0.1 mg/mL of aqueous suspension were prepared. Hydro-dynamic size of nanoparticles was measured and the motion was recorded on NS300 (Malvern), and 0.1 mg/mL of aqueous suspension were prepared for NTA. The surface areas and pore volume were measured through nitrogen sorption measurement. The dried power was kept at 100 °C under vacuum for residual out-gas for 24 hr and nitrogen adsorption and desorption isotherms were acquired using autosorb iQ (Quantachrome) at 77 K. Specific surface area and pore volume were derived by the Brunauer–Emmett–Teller (BET) method. X-ray diffraction (XRD) patterns were recorded on D/ MAX-2500/PC (RIGAKU) diffractometer. The oxidation state of the samples was determined with X-ray source of monatomic and gas cluster ion source using K-Alpha+XPS System (Thermo Scientific). Thermal Gravity Analyzer (TGA) measurement was performed to measure carbon amount in nanoparticles using Q600 (TA instrument) and 15 mg of samples were heated at rate of 10 °C/min in air atmosphere up to 900 °C. Ms values were measured

through superconducting quantum interference device (SQUID) magnetometer (Quantum Design, MPMS3-Evercool), which was equipped with a 7 T superconducting magnet at 300 K. Alternating magnetic field (AMF) were applied by commercial AC applicator (model DM100 by nB (nanoscale Biomagnetics) working at 255 kHz and 200 G field amplitudes. Confocal pictures were obtained using a Leica SP5 Confocal microscope. UV–vis spectroscopy was carried out with a JASCO V-650 UV–vis spectrophotometer.

Thermal annealing under vacuum: The vacuum furnace was fabricated in our lab for ultra-high vacuum conditions. The furnace was composed of a rotary pump, turbo molecular pump (Edwards, HP G1946), vacuum gauge controller (Autovac, GVC 2200), and tube (alumina) furnace. Vacuum condition was held with rotary pump for first 20 minutes to reach at 1×10^{-2} torr, and with turbo pump for second 10 minutes where vacuum gauge indicated 8×10^{-5} torr of vacuum level.

Raman measurement: Raman measurement was performed with a home-built micro-spectroscopy. Briefly, a solid-state laser beam operated at 457 nm (2.71 eV) was focused onto samples within a spot size of $\sim 1 \mu\text{m}$ by using a microscope objective (40 \times , numerical aperture = 0.60) to obtain Raman and PL spectra, respectively. The average power for both measurements was maintained below 1 mW. The backscattered signals were collected with the same objective and guided to a spectrometer combined with a liquid nitrogen-cooled CCD detector. The overall spectral accuracy was better than 1 cm^{-1} for Raman and PL spectra. Samples were prepared on the silicon wafer by dropping 10 μl suspension of samples and dried in dry oven at 60 $^{\circ}\text{C}$ for 1h.

MALDI-TOF analysis: Matrix-assisted laser Desorption/Ionization Time-of-Flight (MALDI-TOF) Mass Spectrometer analysis was conducted to examine the samples dispersed in ethanol. Initially, the sample-ethanol mixture was subjected to centrifugation at 12,000 rpm for 10 minutes. This process enabled the sedimentation of the samples. Following centrifugation, 1 μL of the settled samples was carefully loaded onto the target plate for analysis. The loaded samples were then analyzed using an autoflex speed MALDI-TOF MS (Bruker) instrument. The analysis was performed in the positive reflectron mode utilizing the Laser Desorption/Ionization Mass Spectrometry (LDI-MS) technique.

Liquid-Cell TEM analysis: An In-situ liquid cell TEM holder (Protochips Inc., PoseidonSelect) was used to directly observe the aqueous dispersion of particles. The E-chip, consisting of top and bottom chips with 50nm-thick SiNx windows, was used to enclose water for observing nanoparticles in liquid. In this experiment, liquid thicknesses were set at 150nm and 500 nm, respectively. We flow the solution into the E-chip using a pump (Havard Apparatus, Pump 11 Elite) at a rate of 3 μ l/hr. Once the E-chip was filled, the flow of liquid was stopped and we performed to investigate the dispersion of nanoparticle in the liquid. Movies were recorded in bright field (BF) mode using a Titan TEM (Thermofisher Scientific) operated at 300 keV.

Preparation of SiO₂-NH₂-Pd²⁺ nanoparticles: SiO₂-NH₂-Pd²⁺ NPs were synthesized in a reverse micelle system. First, IGEPAL CO-520 (1.2 mL) and IGEPAL CO-720 (1.2 mL) were dispersed in 20 mL of cyclohexane to make the reverse micelles under magnetic stirring (800 rpm.). Then, Na₂PdCl₄·3H₂O (1.4 M, 25 μ L), aqueous ammonia (28-30%, 200 μ L), 570 μ L of TEOS and 30 μ L of TMSD was sequentially added dropwise under magnetic stirring (800 rpm.), and the reaction was continued at room temperature for 24 h. The product was isolated by adding 20 mL of methanol into the suspension and the settled product was collected by centrifugation (15000 rpm.) followed by three times washing with ethanol.

Synthesis of Col-Pd₂Si@SiO₂ NPs: Powder of SiO₂-NH₂-Pd²⁺ NPs (5 mg) was annealed at 1000 °C for 6 h under high vacuum conditions (8x10⁻⁵ torr). After the vacuum reached the proper level, the temperature was ramped to 1000 °C at the rate of 5 °C/min, and the reaction was continued for 6 h.

Preparation of SiO₂-NH₂-Pd²⁺/Fe³⁺ nanoparticles: SiO₂-NH₂-Pd²⁺/Fe³⁺ NPs were synthesized following the procedure of SiO₂-NH₂-Pd²⁺ NPs with different metal precursors which is a mixture of Na₂PdCl₄·3H₂O (0.7 M) and Fe(Cl)₃ (0.3 M). The reaction was conducted in IGEPAL CO-520 (1.2 mL) and IGEPAL CO-720 (1.2 mL) reverse micelle system under stirring at 800 rpm. Metal precursors, aqueous ammonia (28-30%, 200 μ L), 570 μ L of TEOS and 30 μ L of TMSD was sequentially added dropwise in suspension and the reaction was kept for 24 h. The product was precipitated by methanol and the product was collected by centrifugation (15000 rpm.) followed by ethanol washing.

Long-Term Stability Test: Before starting the long-term stability assessment, the Pd₂Si@SiO₂ nanoparticle suspension was sonicated for 5 minutes to achieve uniform dispersion. Two types of samples were prepared: a 5 mL aliquot in an Eppendorf tube for dynamic light scattering (DLS) analysis and a 2 mL aliquot in a cuvette for photographic documentation. The cuvette sample was left undisturbed at room temperature to observe any sedimentation over time. Each week, 1 mL of supernatant was carefully extracted from the 5 mL suspension for DLS measurements, consistently showing the same particle concentration and size in every sample. While the 2 mL cuvette sample was used for imaging, providing a detailed evaluation of dispersion stability over time. Similarly the data was obtained after keeping the sample undisturbed for 6 month.

Cellular cytotoxicity: The cytotoxicity of various concentrations of **FeSi-Pd₂Si@SiO₂ NPs**, nanoparticles was evaluated using the Cell Counting Kit (CCK, Countess II, Invitrogen, Thermo Fisher Scientific) by incubating with cell-lines: MDA-MB-231 (metastatic human breast adenocarcinoma)] for 12 hours. In a 96-well plate, 5000 cells per well were cultured in 100 μL of DMEM supplemented with 10% FBS at 37°C and 5% CO₂ atmosphere. After 24 hours of seeding, cells were incubated with various concentrations (10, 20, 100, 200 and 500 μg/mL) of FeSi-Pd₂Si@SiO₂ NPs for 12 hours. Subsequently, the cells were washed thrice with phosphate-buffered saline (PBS), and cell viability was measured using a CCK assay.

AMF induced [Pd]-catalyzed deprotection catalysis: AMF-induced [Pd]-catalyzed deprotection reaction was carried out using 1 mg/mL of **FeSi-Pd₂Si@SiO₂ NPs**. The MDA-MB-231 cells were cultured in DMEM-medium (1 mL) in cell-plates (50,000 cells/mL) for 24 hours at 37 °C (5% CO₂). Subsequently, the cell media was replaced with fresh media containing **FeSi-Pd₂Si@SiO₂ NPs** (1 mg/mL in DMEM) and incubated for an additional 3 h. Following this, the cell media was discarded, and the cells were washed with PBS (three times) to eliminate extracellular **Pd₂Si@SiO₂ NPs**. Next, the cells were incubated with fresh media containing Poc-Rho (1 mM) for 1 h. Then, the cells were exposed to AMF with a strength of 200 G and a frequency of 255 KHz for 3 h. After the reaction, the cells underwent two washes with PBS and were then treated with NucBlue™ (Invitrogen). Following this, cell harvesting was performed using trypsin/EDTA, and the cells were redispersed in PBS buffer.

The intracellular presence of the fluorescent compound was analyzed using flow cytometry, specifically in FITC-A (for cytosol) and Pacific Blue-A (for the nucleus). Data acquisition was conducted using the LSR Fortessa instrument.

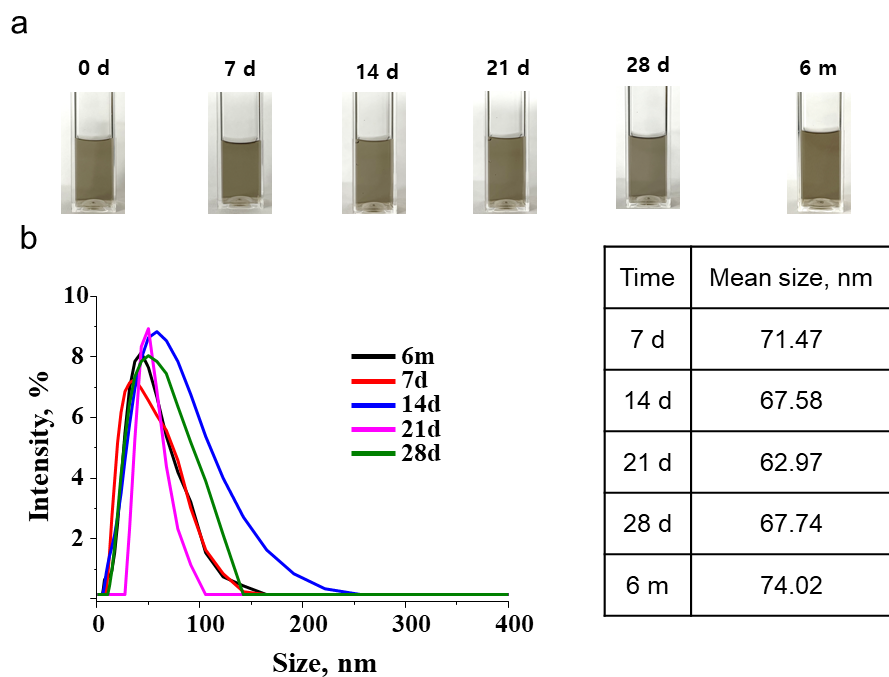


Fig. S1. (a) Optical images of time-dependent dispersion stability test of $\text{Pd}_2\text{Si}@\text{SiO}_2$ in aqueous solution (b) corresponding time dependent dynamic light scattering (DLS) analysis of $\text{Pd}_2\text{Si}@\text{SiO}_2$ reflecting particles are highly colloidal nature, with minimal changes in size, upto 6 month of time period.

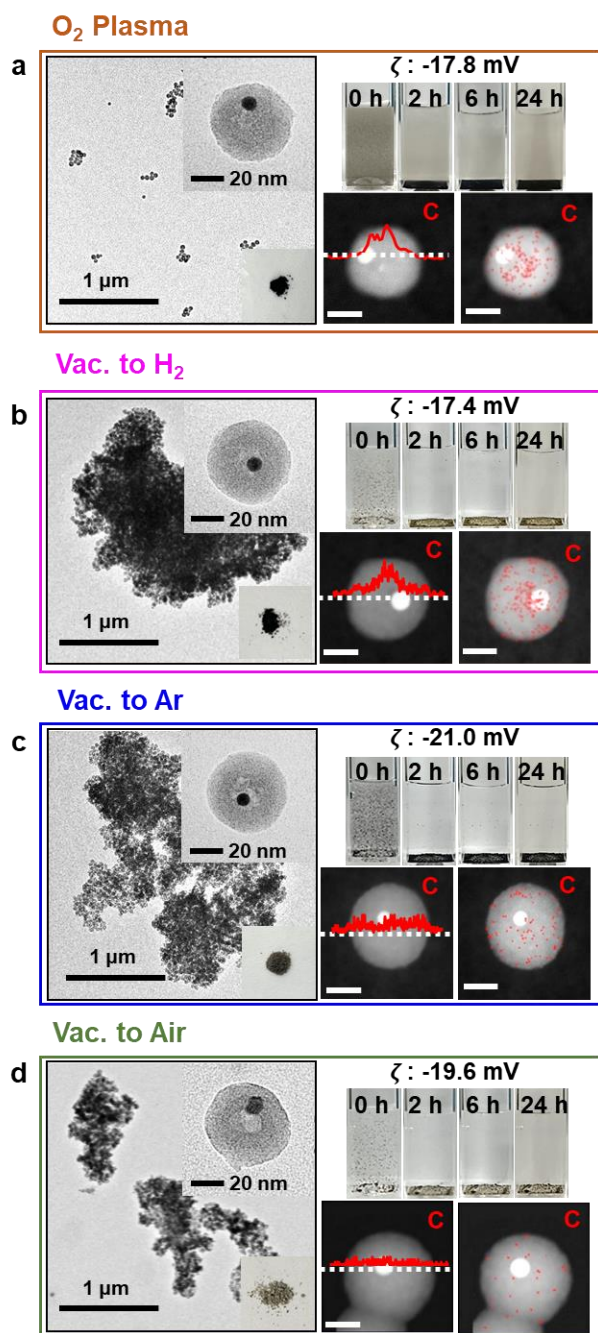


Fig. S2. Additional treatment of Pd₂Si@SiO₂ NPs in different gas environment. TEM image (inset: powder photo), EDS-based elemental mapping and line-profiling, dispersity test and zeta potential of Pd₂Si@SiO₂ NPs treated under (a) O₂ plasma, (b) H₂, (c) Ar, (d) Air. Under air, H₂, and Ar environment the formation of similar bulk fused structures of silica NPs was observed.

Extended discussion regarding Fig. S1: To reveal the role of carbon species in the aqueous dispersity, as synthesized Pd₂Si@SiO₂ powders were first, post-treated with O₂ plasma, causing the selective removal of surface carbonaceous species, as confirmed by the EDS-based elemental mapping/line-profiling (Fig. S1a) and Fig. 2c (in manuscript). It in turn caused the change in surface zeta-potential and inferior colloidal stability of Pd₂Si@SiO₂ (Fig. S1a), also verified by the TEM images showing

slightly aggregated NPs. Alternatively, annealing of $\text{Pd}_2\text{Si@SiO}_2$ powders under different gas environments (H_2 , Ar, air) caused possible chemical degradation of carbonaceous skin, causing NP aggregation (Fig. S1b-d and Fig. 2c in manuscript). These post-synthetic treatment experiments verified the crucial role of carbonaceous skin in determining the colloidal stability of the NPs.

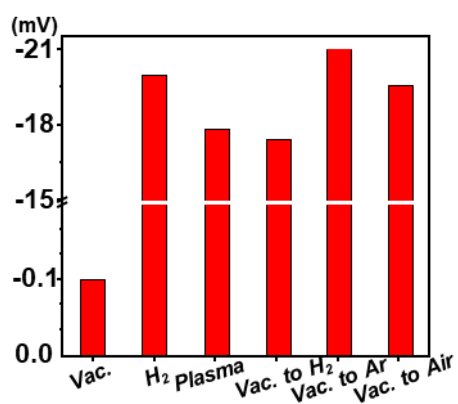


Fig. S3. Zeta Potential of $\text{Pd}_2\text{Si@SiO}_2$ NPs after additional treatment under different gaseous environments.

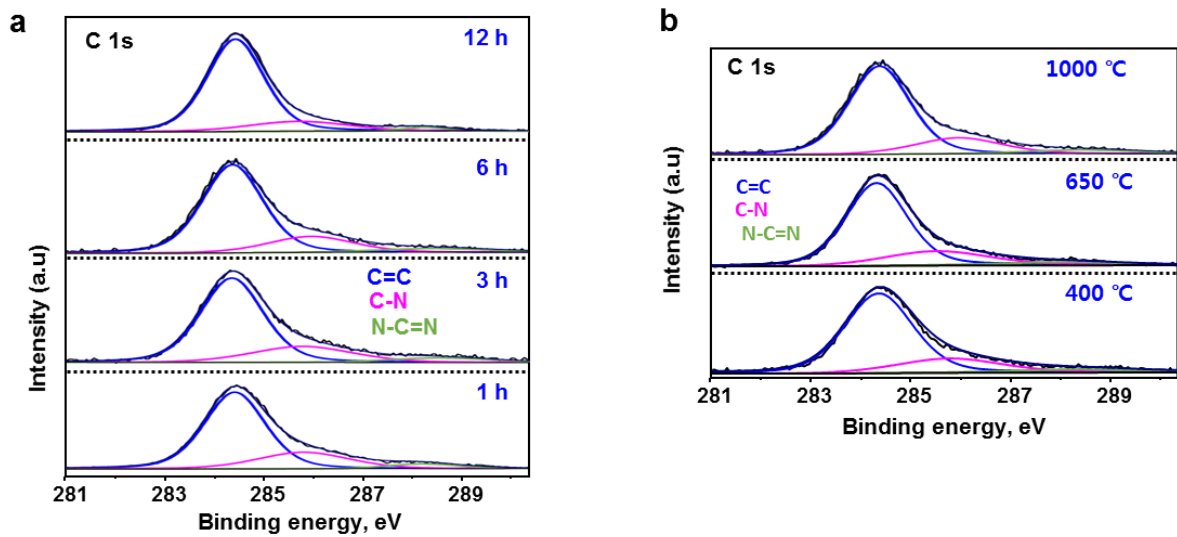


Fig. S4. XPS spectrum of (a) time course and (b) temperature variation from $\text{SiO}_2\text{-NH}_2\text{-Pd}^{2+}$.

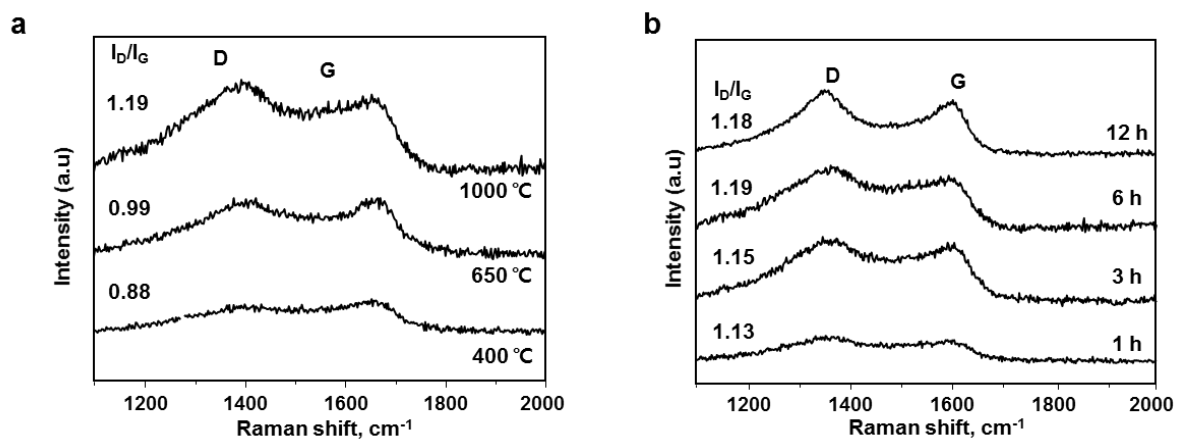


Fig. S5. Raman spectrum of (a) time course and (b) temperature variation from $\text{SiO}_2\text{-NH}_2\text{-Pd}^{2+}$.

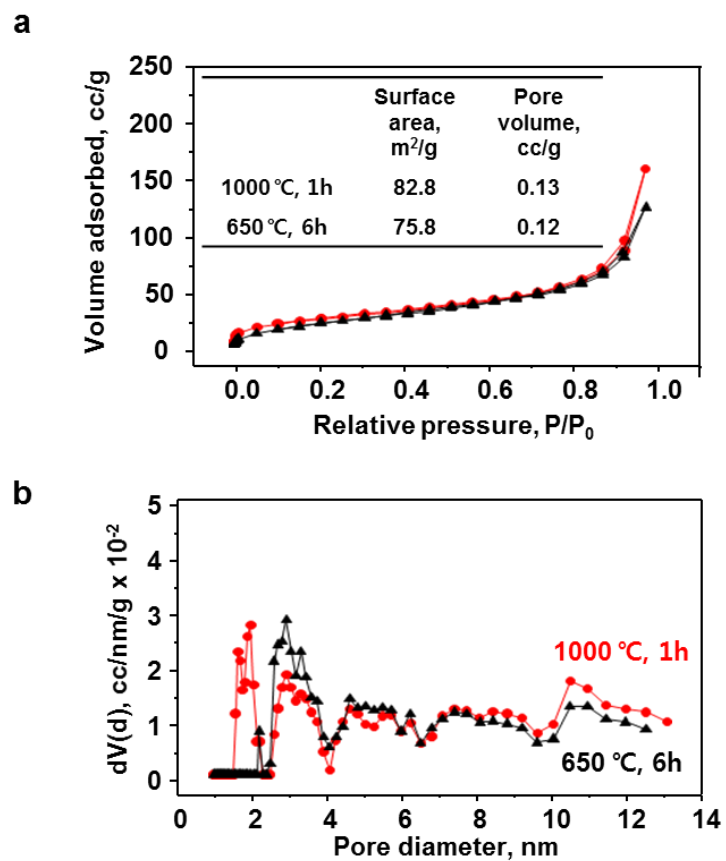


Fig. S6. (a) BET surface area time course and (b) BJH pore size distribution plots of $\text{SiO}_2\text{-NH}_2\text{-Pd}^{2+}$ NPs treated under vacuum at 1000°C for 1 h and 650°C for 6 h.

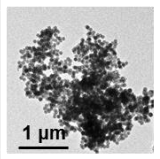
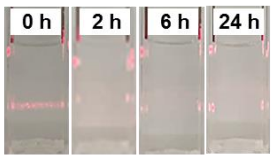
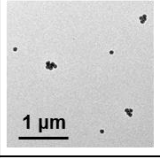
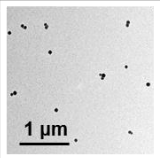
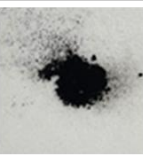
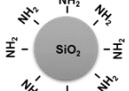
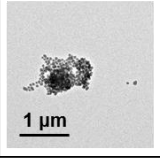
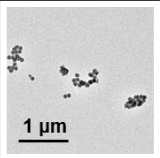
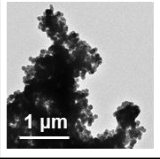
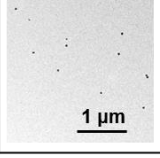
Nanoparticles	TEM image	Powder	Dispersity test
 SiO ₂	 1 μm		
 SiO ₂ @SiO ₂ -NH ₂ @SiO ₂	 1 μm		
 SiO ₂ -NH ₂	 1 μm		
 SiO ₂ @SiO ₂ -NH ₂	 1 μm		
 SiO ₂ @dopamine	 1 μm		
 SiO ₂ -CH ₃ -Pd ²⁺	 1 μm		
 SiO ₂ -NH ₂ -Pd ²⁺	 1 μm		

Table S1. Dispersity test of the silica nanoparticles with different compositions treated under vacuum at 1000 °C for 6 h. This study verified the crucial role of interior Pd(II) ions and aminoalkyl-groups on self carbo-passivation process and in turn colloidal dispersity of the resulting NPs (last row). All other compositions afforded aggregated NPs.

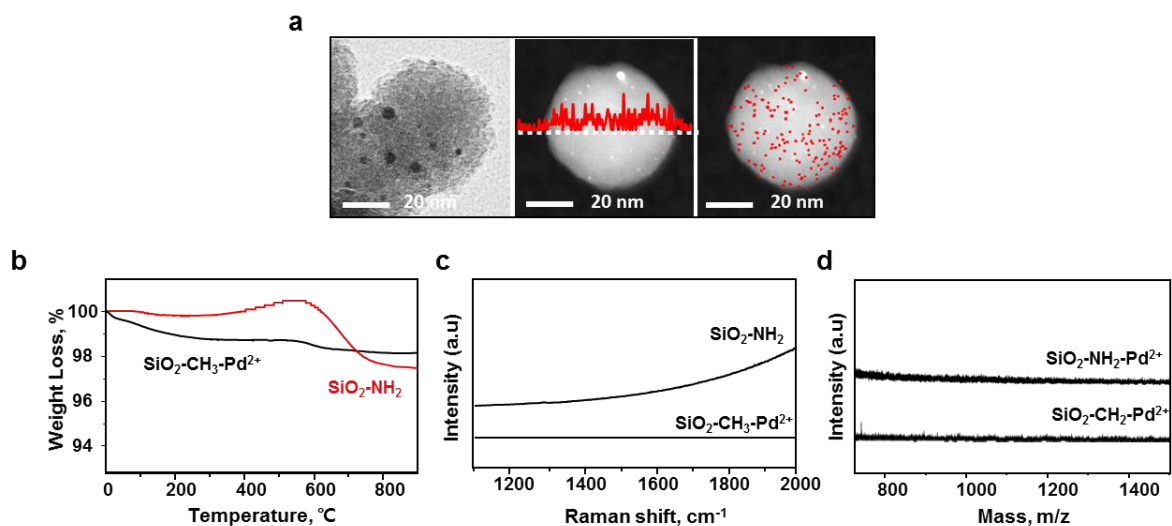


Fig. S7. TEM image and HAADF-STEM based EDS elemental line-profiling and -mapping of $\text{SiO}_2\text{-CH}_3\text{-Pd}^{2+}$ (no amine) after vacuum annealing at 1000 °C for 6 h. TGA profiling (b), Raman spectra (c), and MALDI spectra of $\text{SiO}_2\text{-CH}_3\text{-Pd}^{2+}$ (no amine) and $\text{SiO}_2\text{-NH}_2$ (no Pd) after vacuum annealing at 1000 °C for 6 h. These alternative compositions did not create high-mass graphitic species on the silica NP surface and failed to lead carbo-passivation.

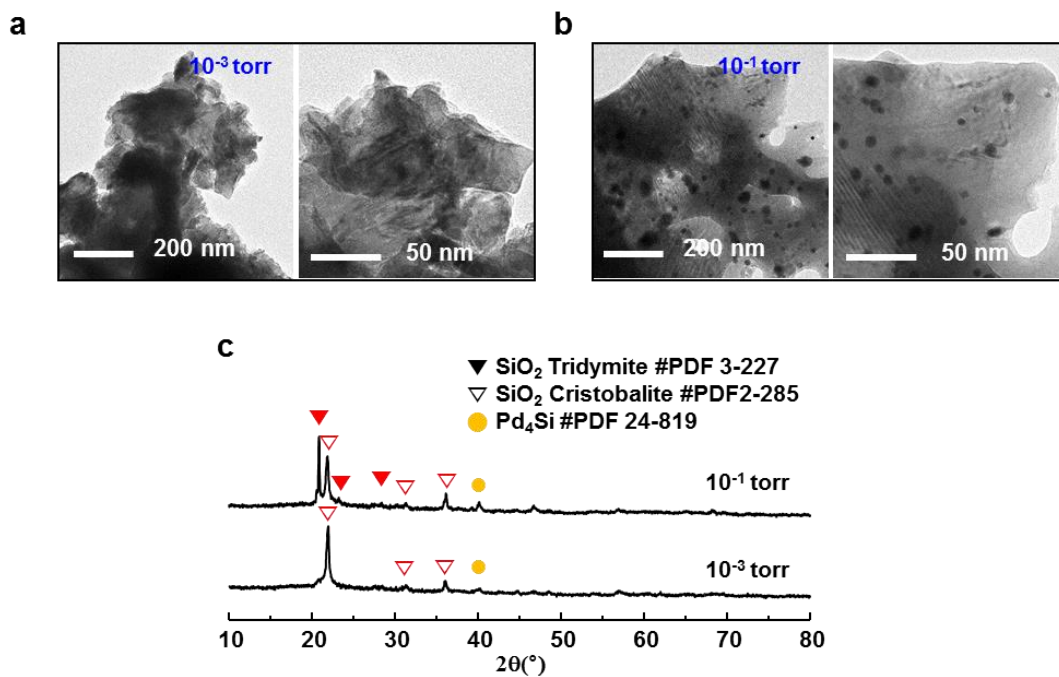


Fig. S8. Vacuum treatment of $\text{SiO}_2\text{-NH}_2\text{-Pd}^{2+}$ NPs at $1000\text{ }^{\circ}\text{C}$ at different vacuum levels. TEM images of vacuum-treated samples at 10^{-3} torr (a) and 10^{-1} torr (b). (c) Corresponding XRD spectra. These alternative vacuum conditions generated bulk crystalline silica phase.

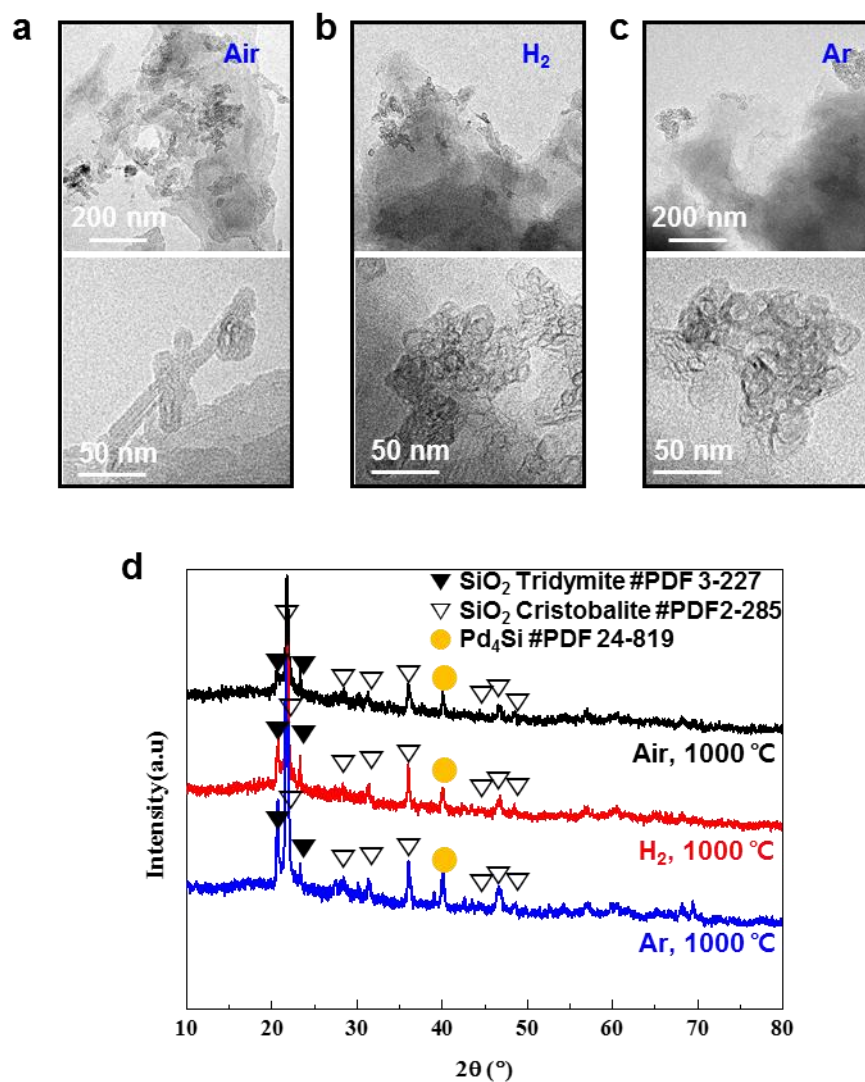


Fig. S9. Treatment of $\text{SiO}_2\text{-NH}_2\text{-Pd}^{2+}$ NPs at $1000\text{ }^\circ\text{C}$ under different gas conditions. TEM images of the sample treated under Air (a), H_2 (b), and Ar (c) atmospheres. (d) Corresponding XRD spectra. These alternative annealing conditions under different environments (replacing vacuum) generated crystalline bulk silica phase.

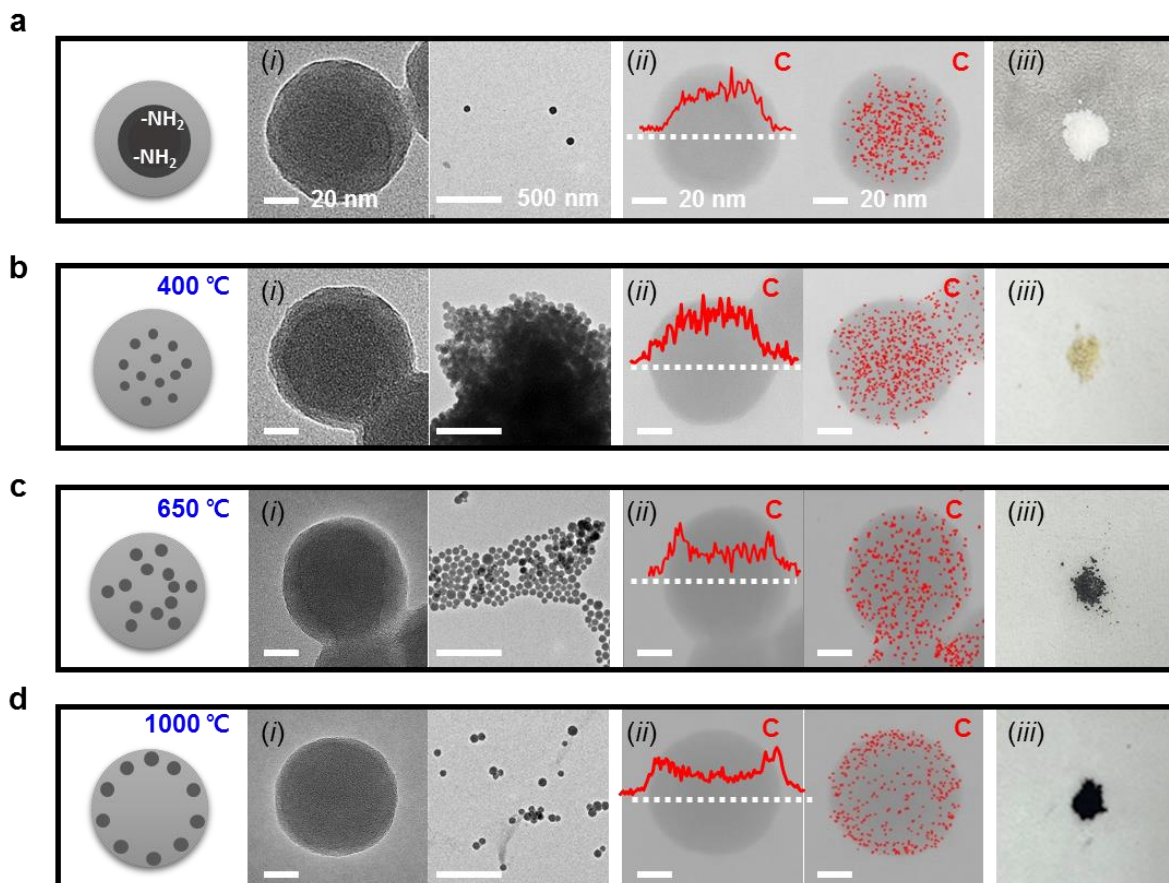


Fig. S10. TEM images (i), HAADF-STEM EDS-based elemental line profiling/mapping (ii) and digital photographs of powder form (iii) of $\text{SiO}_2\text{-NH}_2$ NPs (no Pd) before (a) and after vacuum annealing at different temperatures. A high temperature ($1000\text{ }^\circ\text{C}$) was essential for generating and diffusing carbon species onto the NP surface.

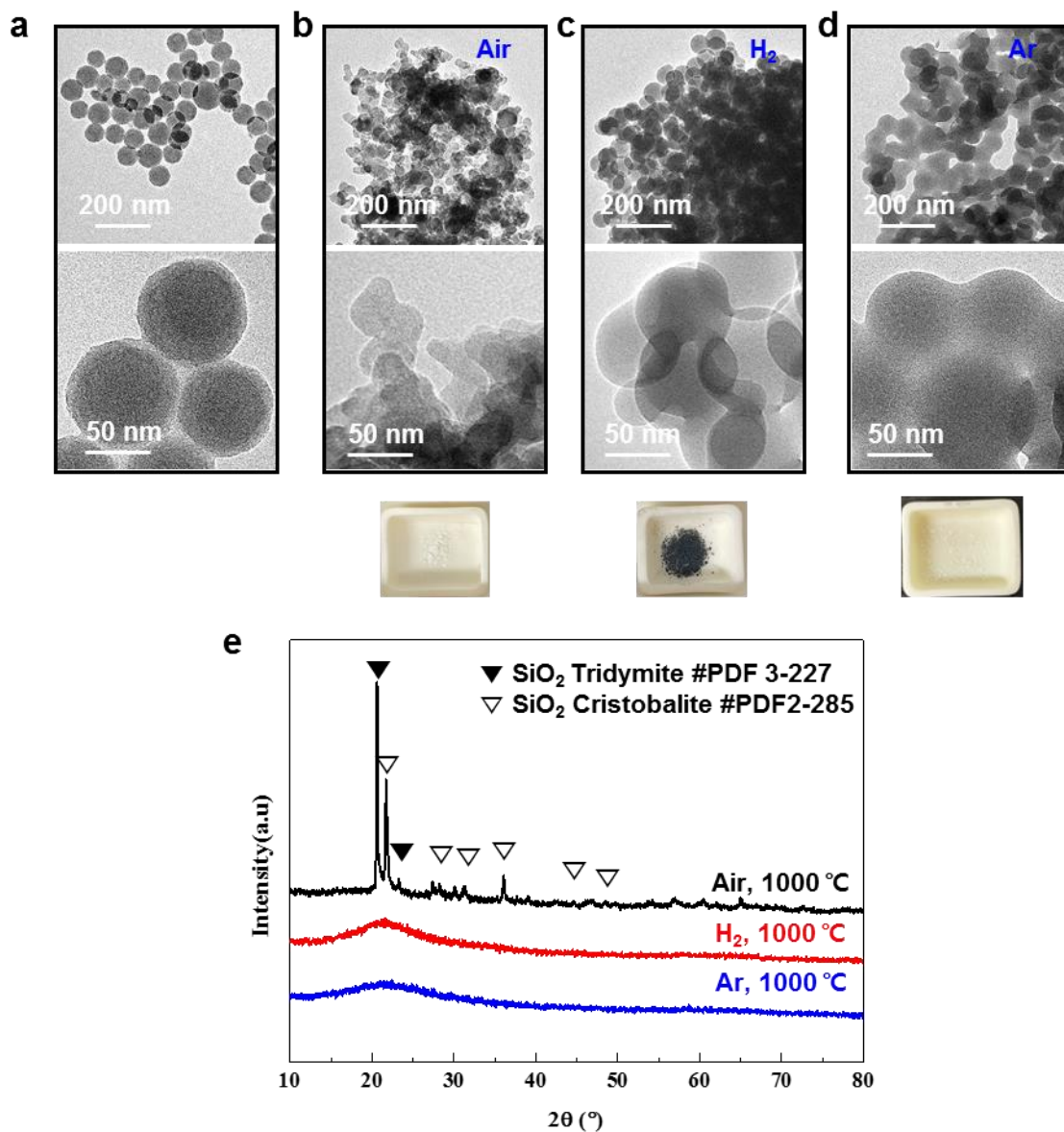


Fig. S11. TEM images of $\text{SiO}_2\text{-NH}_2$ NPs (no Pd) before (a) and after annealing at 1000 °C under Air (b), H_2 (c), and Ar (d) environments. Corresponding digital photographs below TEM images (e) Corresponding XRD spectra. These alternative annealing conditions generated fused NPs and bulk crystalline silica phase (air annealing).

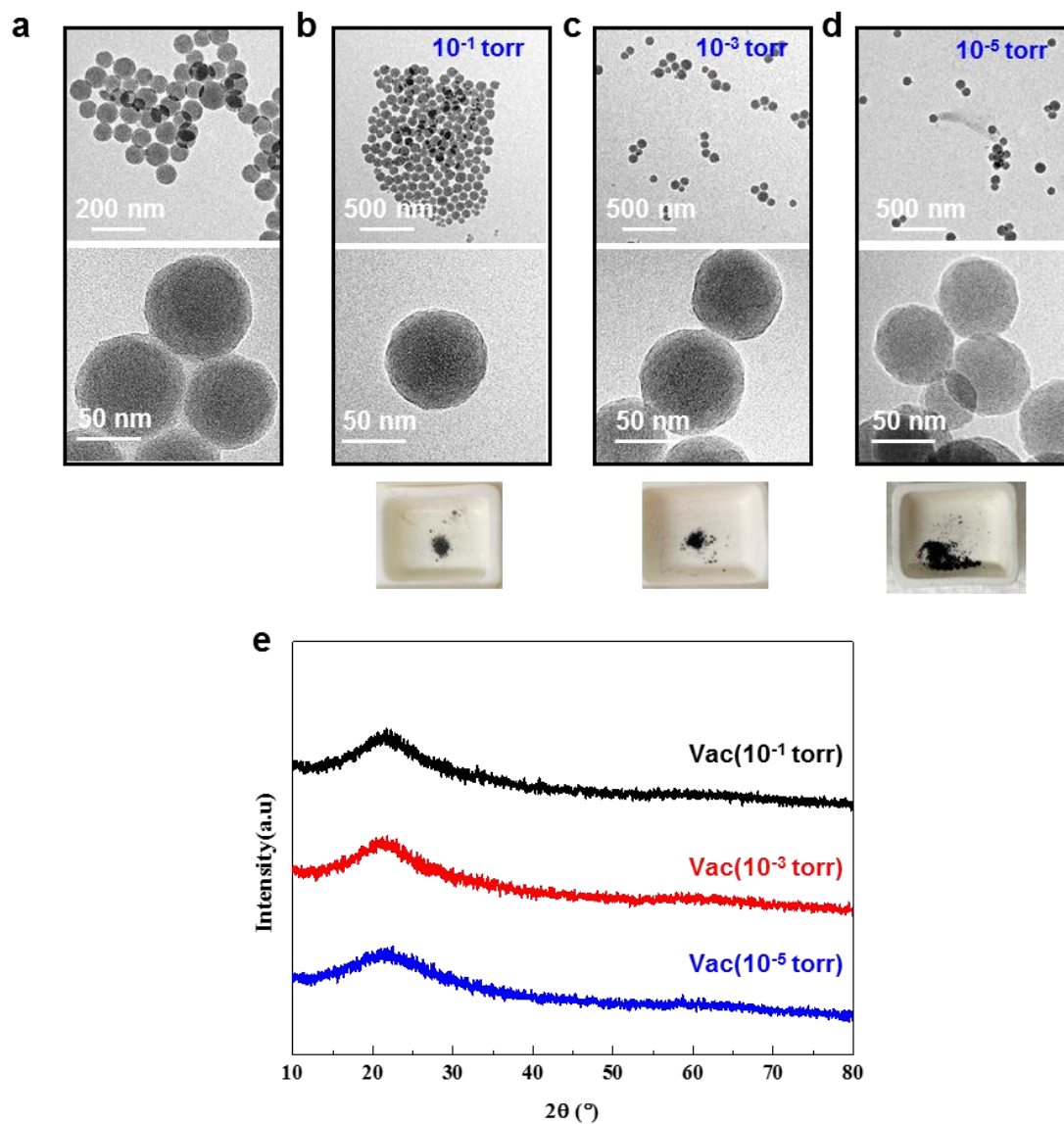


Fig. S12. TEM images of $\text{SiO}_2\text{-NH}_2$ NPs (no Pd) before (a) and after annealing at 1000 °C at different vacuum levels (b-d).

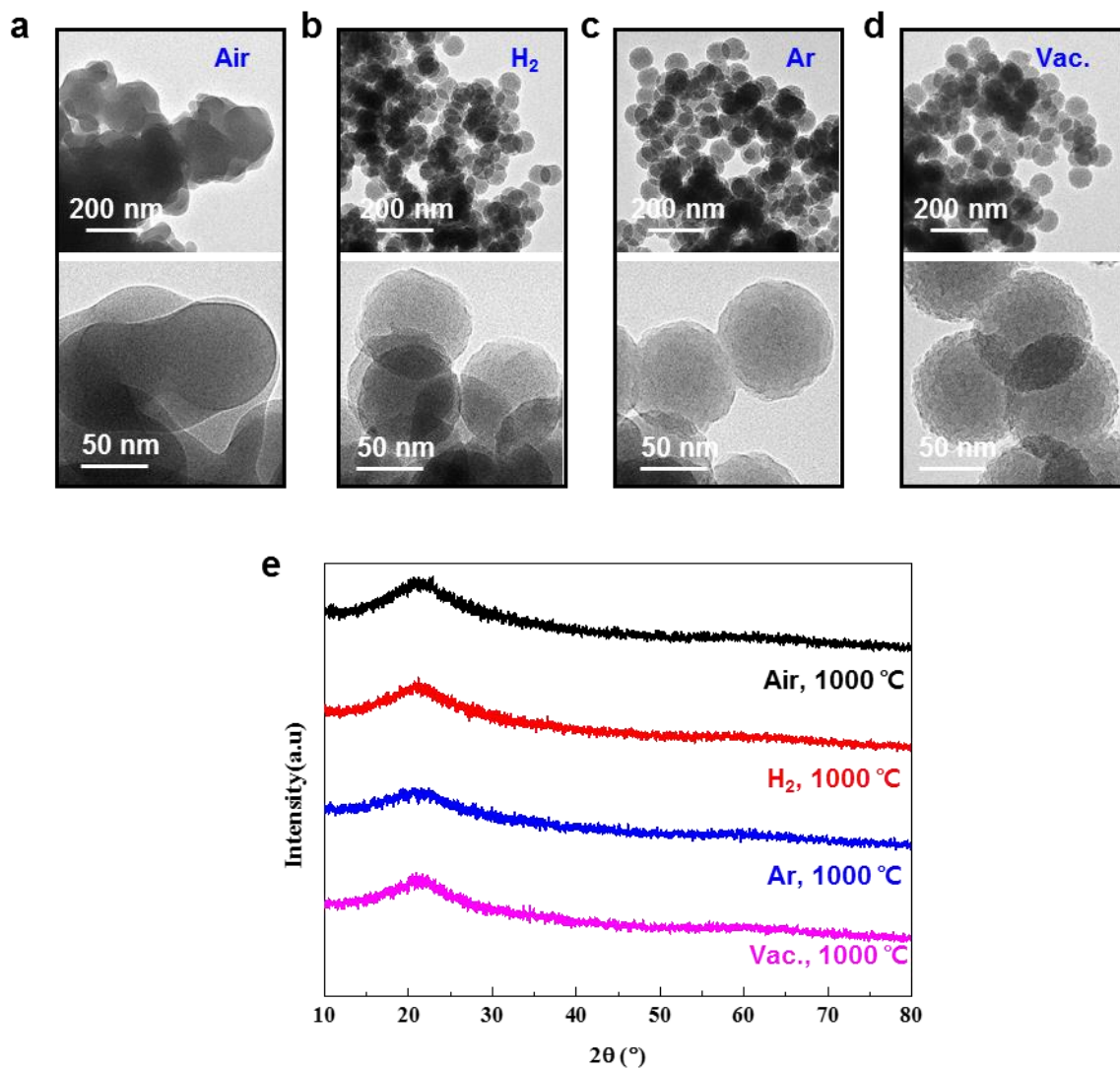


Fig. S13. Annealing of SiO₂ NPs at 1000 °C under different environments. TEM images (a-d) and corresponding XRD spectra (e).

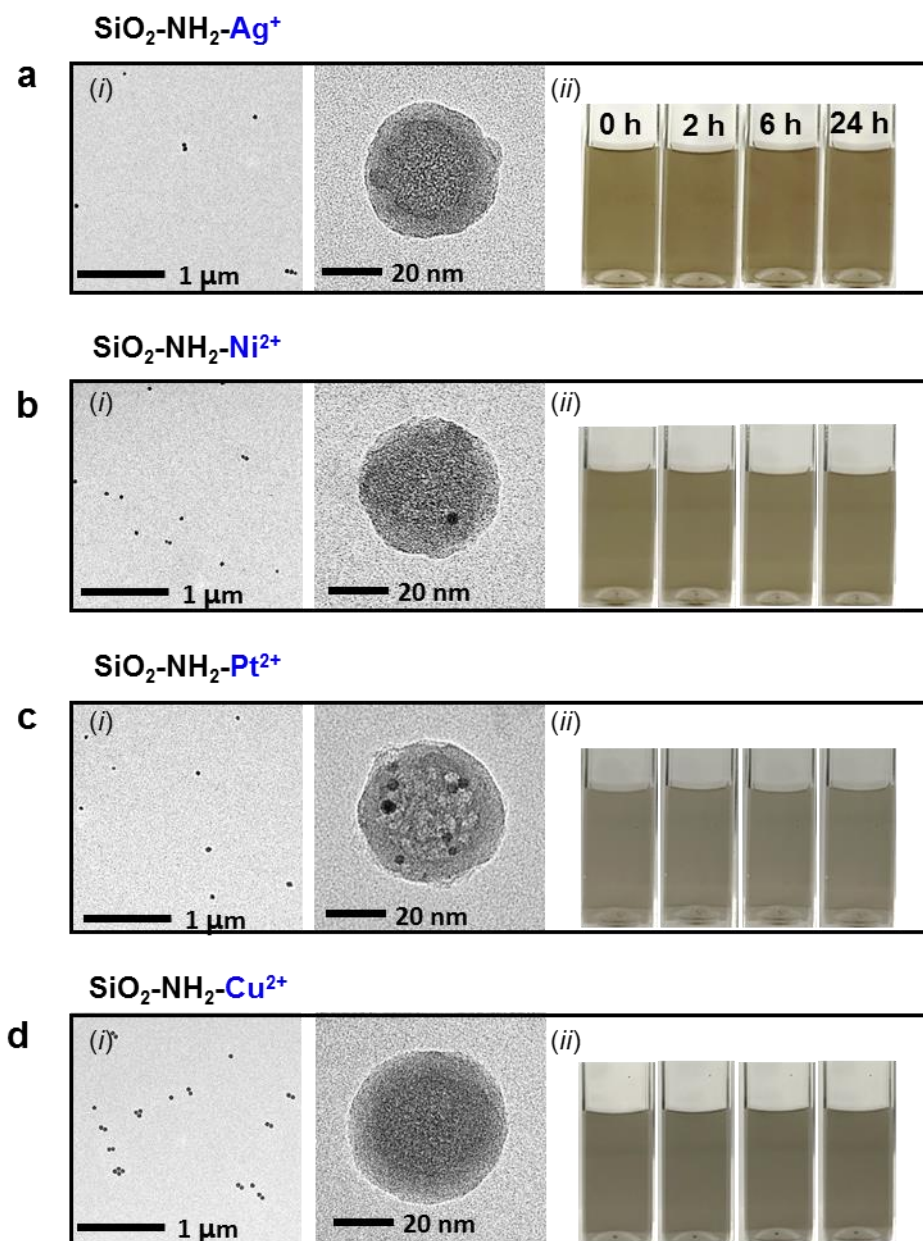


Fig. S14. Vacuum-treatment of $\text{SiO}_2\text{-NH}_2\text{-M}$ NPs ($M =$ (a) Ag^+ , (b) Ni^{2+} , (c) Pt^{2+} , (d) Cu^{2+}) at $1000\text{ }^\circ\text{C}$. (i) TEM images and (ii) dispersivity test of vacuum-treated samples.

Before reaction

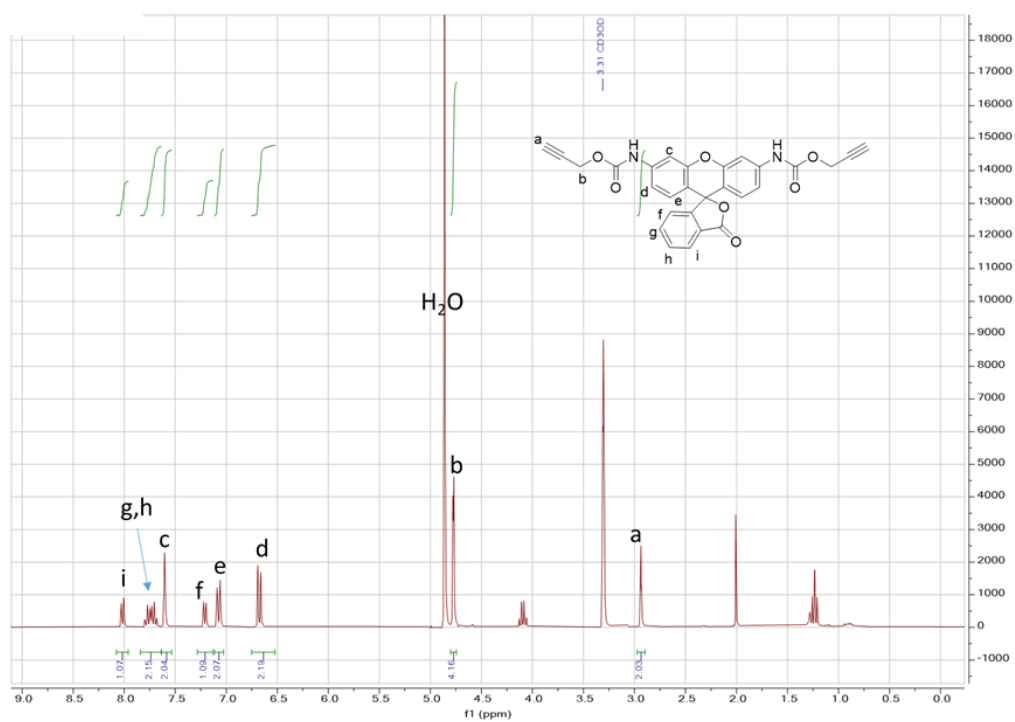
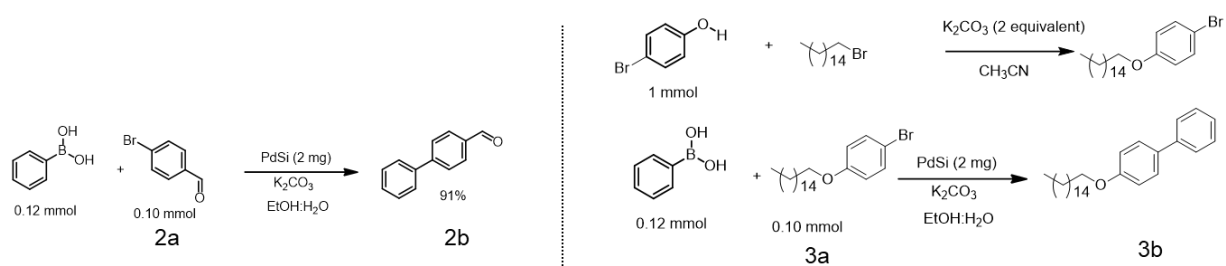


Fig. S15. ^1H NMR spectra of before reaction.

Table S2: Suzuki-Miyaura coupling using Pd₂Si@SiO₂.



Entry	Catalyst	Solvent	Time (h)	Conversion (%)	Product Yield (%)
2a	Pd ₂ Si@SiO ₂	EtOH: H ₂ O (1:1)	12 h	91%	91%
3a	Pd ₂ Si@SiO ₂	EtOH: H ₂ O (1:1)	12 h	ND	ND

Phenylboronic acid (0.12 mmol), PdSi (2 mg), aryl bromide (0.1 mmol) base (1 equivalent), EtOH:H₂O (1 mL), 60 °C for 12 h, Yield was calculated using 1,3,5 trimethoxy benzene as a internal standard.

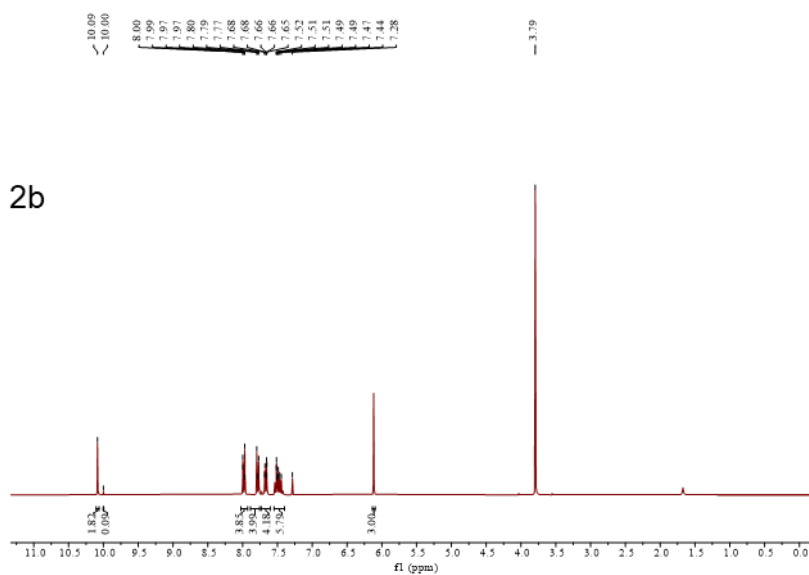


Fig S16. ¹H NMR spectra of 2b in CDCl₃.

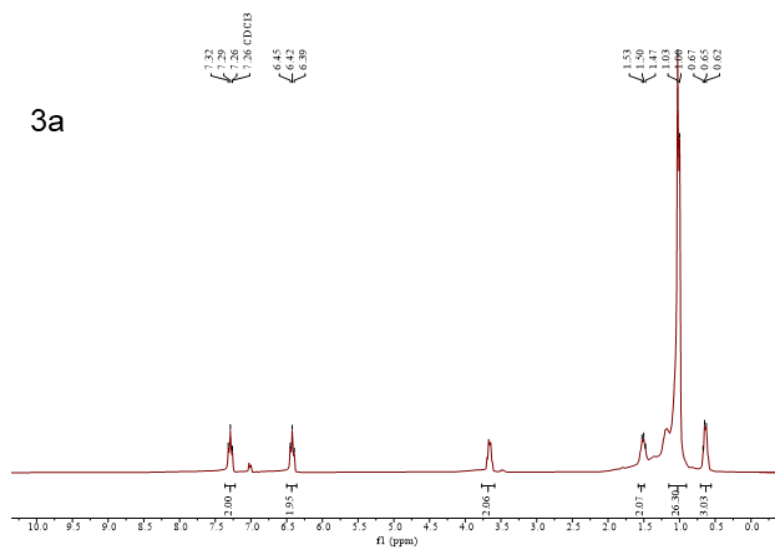


Fig S17. ^1H NMR spectra of 3a in CDCl_3 .

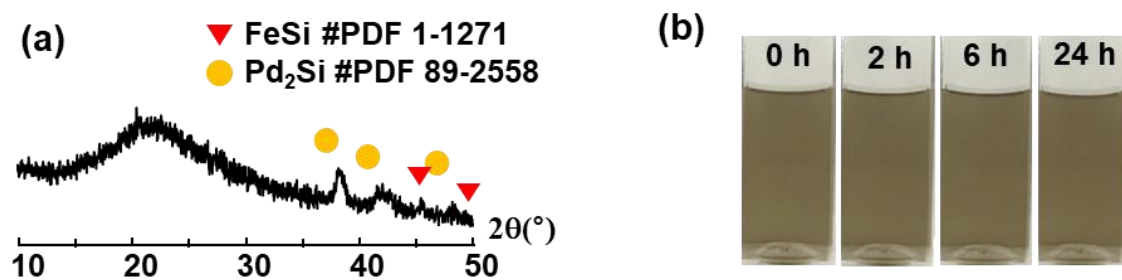


Fig. S18. (a) XRD data of **FeSi-Pd₂Si@SiO₂** NPs, (b) dispersivity test of **FeSi-Pd₂Si@SiO₂** NPs.

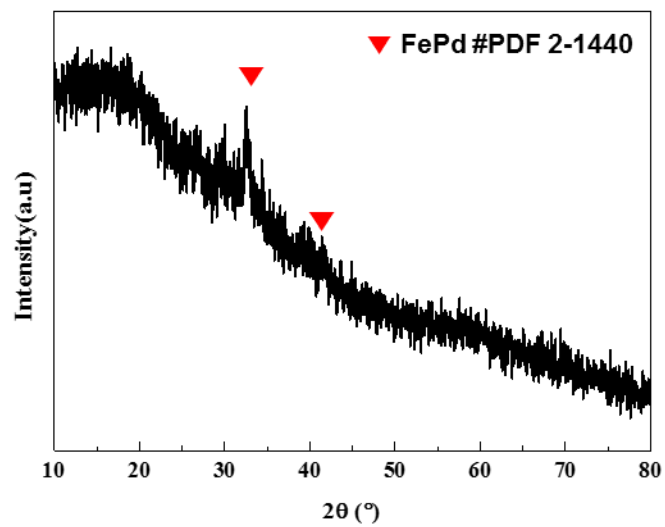


Fig. S19. XRD spectrum of $\text{SiO}_2\text{-FePd}$ NPs treated under H_2 at $800\text{ }^\circ\text{C}$

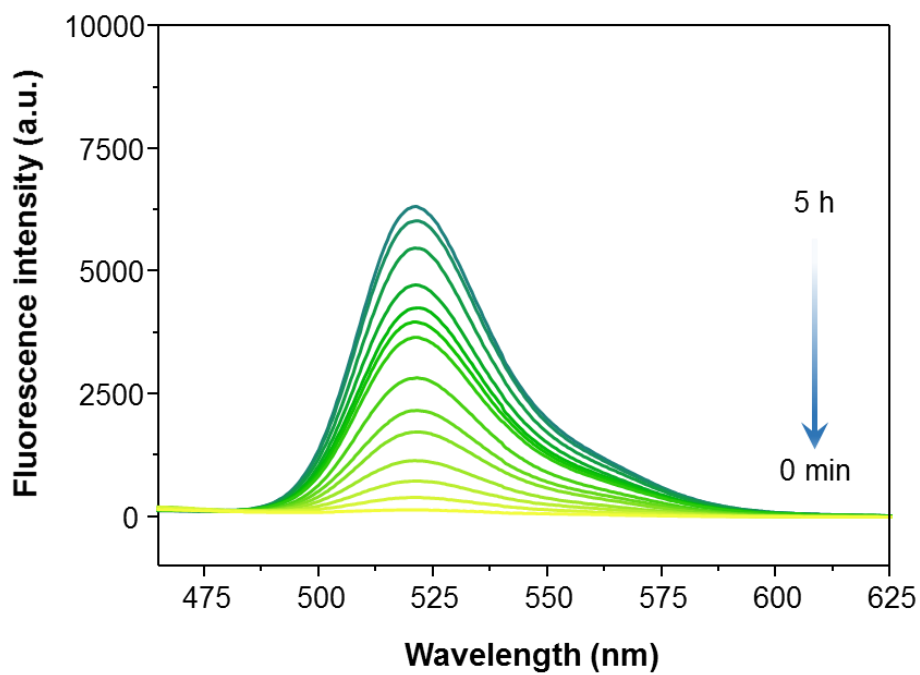


Fig. S20. Study of reaction kinetics of deprotection reaction catalyzed by **FeSi-Pd₂Si@SiO₂** NPs by the change in fluorescence intensity with different times.

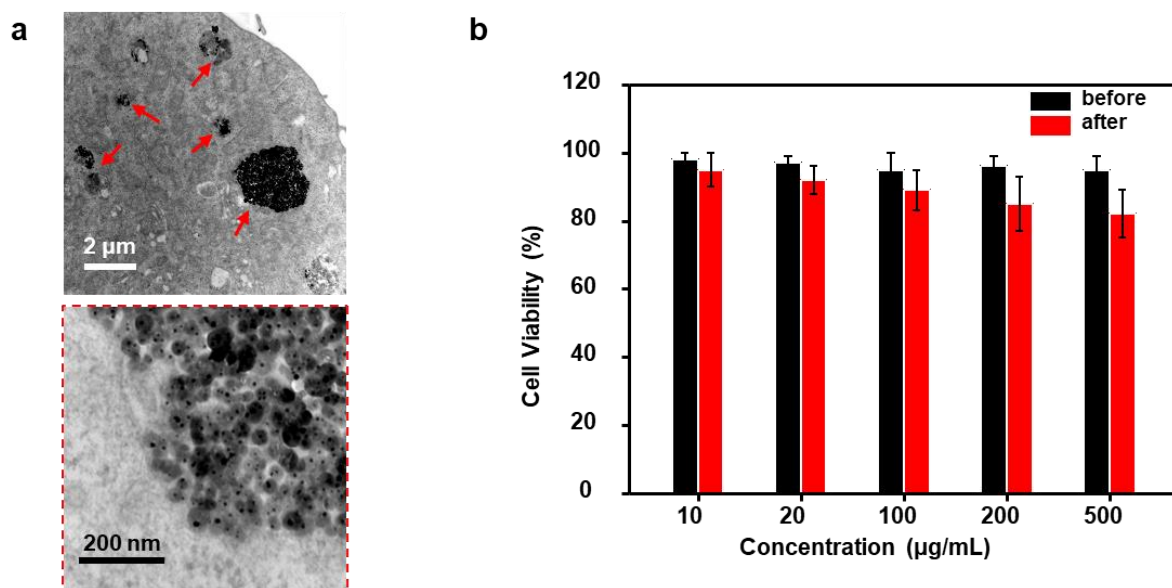


Fig. S21. (a) TEM images of fixed and sectioned cells internalized with **FeSi-Pd₂Si@SiO₂** NPs, (b) Cell viability results of NPs-treated MDA-MB-231 cells

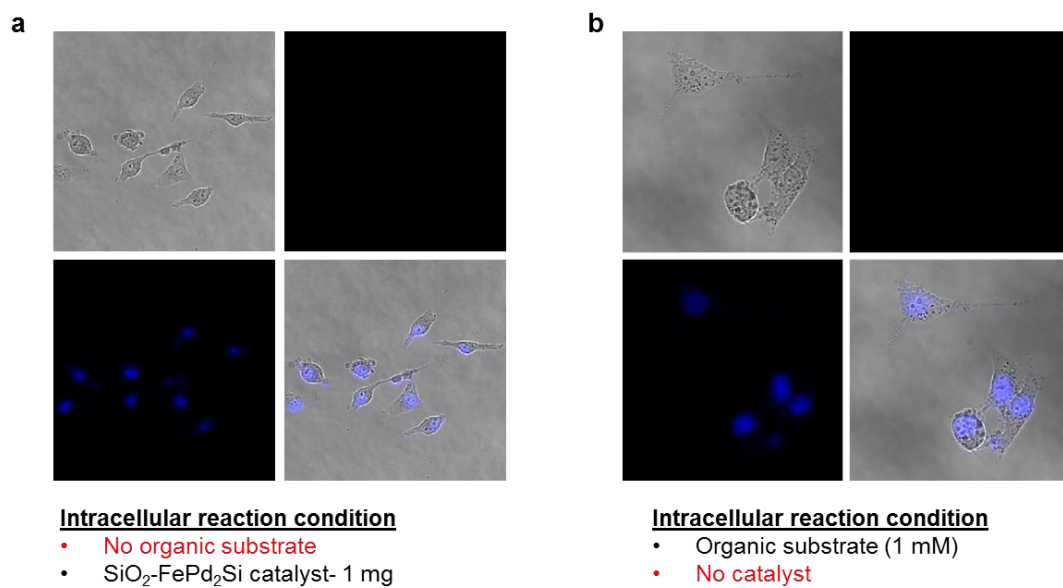


Fig. S22. Bright-field and fluorescence images of MDA-MB-231 cells after reaction under AMF each condition. (a) No organic substrate, (b) No catalyst.